Numerical Analysis of the Optimal Exercise Boundary of an American Put Option

by

Per Lindberg Gunnar Marcusson Gustav Nordman

Internal Report No. 2002:7

May 2002

UPPSALA UNIVERSITET
Inst. för informationsteknologi
Avd. för teknisk databehandling

UPPSALA UNIVERSITY
Information Technology
Dept. of Scientific Computing

Sammanfattning

Randen till fortsättningsområdet, f_{opt}, för en amerikansk säljoption studeras genom att lösa Black-Scholes partiella differentialekvation numeriskt. Vi använder oss av Crank-Nicolsons finita differens schema och sedan en enkel jämförelsefunktion.

Vi jämför sedan f_{opt} med kända egenskaper för existerande modeller av det asymptotiska beteendet, både i slutet av giltighetstiden och för den oändliga säljoptionen.

Eftersom det ej finns någon analytisk funktion som beskriver randen till fortsättningsområdet anpassar vi polynom av olika grader till den numeriska lösningen. Vi undersöker sedan hur polynomens koefficienter beror av σ (volatiliteten) och r (räntan).

Abstract

The optimal exercise boundary for an American put option is studied by solving the Black-Scholes partial differential equation numerically. This is carried out using the Crank-Nicolson scheme and then finding the optimal exercise boundary using a simple comparison algorithm.

We then investigate if our solution follows the known mathematical properties of the boundary. There is no analytical solution to the problem, but the asymptotical behavior of the optimal exercise boundary is known when approaching expiry and when time to expiry goes to infinity.

Since no analytical solution is known, we approximate the optimal exercise boundary with a polynomial. Having done this we examine how the coefficients vary for the involved parameters σ (volatility) and r (interest rate).

Contents

1 Introduction **2**

2 Problem Definition **2**

2.1 Formulae 2

2.2 Problem Description 3

3 Numerical Pricing of the American Put **5**

3.1 Time discretization of the American Put 5

3.2 Numerical method 5

3.3 Boundary Conditions 7

3.4 Finding the Optimal Exercise Boundary 7

3.5 Accuracy of the numerical method 9

3.6 Performance 9

4 Optimal Exercise Analysis **10**

4.1 Properties far from maturity 10

4.2 Properties near maturity 13

4.3 Curve fitting of the numerical solution 15

5 Discussion **21**

5.1 Far from maturity 21

5.2 Near maturity 21

5.3 Curve fitting 21

1 Introduction

American options are widely traded throughout the world. This even though European options are better mathematically described. In fact the pricing problem of American options has not yet been solved analytically.

We have studied the properties of the American put option. This is a financial derivative which gives the holder the right (but not the obligation) to sell an asset, e.g. a stock, for a pre-specified price up until a certain time, the so called expiry date, here denoted by T.

We started by comparing the American put to the European. They are quite similar and differ only in the fact that European options can only be exercised at the expiry date.

Using these similarities we were able to give a good numerical approximation of the American put. This in turn gave us an opportunity to analyze the optimal exercise boundary. It describes, depending of the current price of the underlying asset, if one should continue to hold or exercise the option.

2 Problem Definition

One of the fundamental building blocks of option pricing is the *Black-Scholes equation* (Theorem 2.2) describing the European option. Without this equation the rapid development of option markets worldwide had not been possible. In this section we will first state the basic formulae and then define the scope of our investigation.

2.1 Formulae

Definition 2.1 *The* **Black-Scholes market model** *consists of two assets with dynamics given by*

$$dB(t) = rB(t) \tag{1}$$
$$dS(t) = \alpha S(t)dt + \sigma S(t)dW(t) \tag{2}$$

where r, α and σ are deterministic constants. B is a risk free asset (Bond), S is a (more or less) risky asset (Stock), r is the interest rate, α is the local mean rate of return and σ is the volatility, which describes the magnitude of the fluctuations of S. The term dW is a Wiener process.

Theorem 2.2 (Black-Scholes equation) *Assume that the market is specified by 2.1 and that we want to price a contingent claim of the form* $\mathcal{X} = \Phi(S(T))$. *Then the only pricing function of the form* $\Pi(t) = F(t, S(t))$ *which is consistent with the absence of arbitrage is when* F *is the solution of the following boundary value problem in the domain* $[0, T] \times R_+$.

$$F_t(t,s) + rsF_s(t,s) + \frac{1}{2}s^2\sigma^2(t,s)F_{ss}(t,s) - rF(t,s) = 0 \tag{3}$$

$$F(T,s) = \Phi(s) \tag{4}$$

Equations (3) and (4) can be solved using the Feynman-Kač representation formula (see [1]), this gives us the arbitrage free price for the European

$$F(t,s) = e^{-r(T-t)}E^Q_{t,s}[\Phi(S(T))] \tag{5}$$

Both the American and the European option have the contract function

$$\Phi(S(T)) = (K - S)^+ = \max(K - S, 0), \tag{6}$$

where K is the strike price.

In order to price the American put option we have to solve the optimal stopping problem

$$\max_{\tau}\left(E^Q\left[e^{-r\tau}\Phi(S_\tau)\right]\right), \quad \tau \in [0,T],$$

where $E^Q[\ ]$ denotes the expected value under the probability measure Q, defined such that S has the dynamics

$$dS(t) = rS(t)dt + \sigma\left(t, S(t)\right)S(t)dW(t)$$

under Q.

2.2 Problem Description

Our main goal is to analyze the *optimal exercise boundary*, that separates the area where one should continue to hold the option and the area where one should exercise it.

This is done by observing the point of intersection (s_i) on the s-axis where the price F becomes identical to the contract function for all $s < s_i$. This is

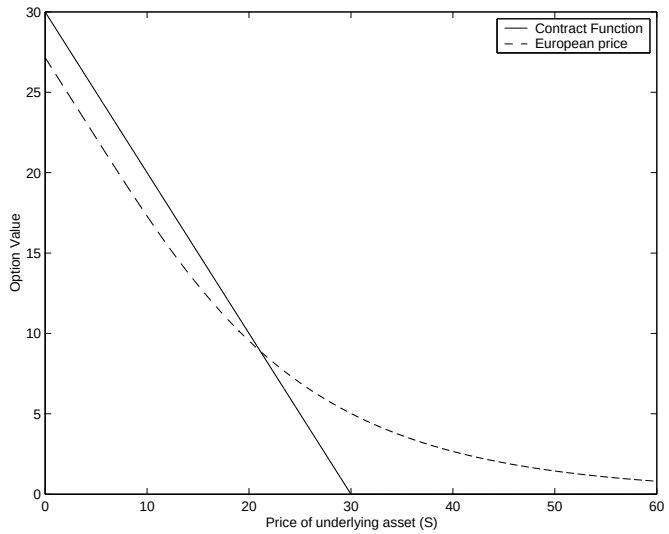

Figure 1: Contract function $y = (K - S)^+$ and price function for a European put option.

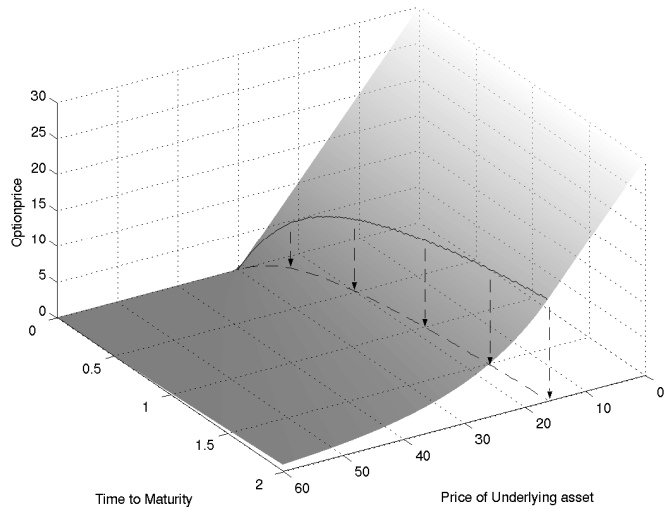

Figure 2: Price surface for an American put and the optimal exercise boundary.

due to the fact that the American put option always must be worth at least $\Phi(s(t))$ since one can exercise it at any time.

One can roughly say that the point of optimal exercise occurs where the European option intersects the payoff function in figure 1. For the American put this intersection never occurs since, as stated earlier, the prices are identical

for $s(t) < s_i(t)$.

The points $s_i(t)$ $\forall t \in [0, T]$ gives us the optimal exercise boundary curve $f_{opt}(t)$. When $s(t) < f_{opt}(t)$ one should exercise the put, on the other side, $s(t) > f_{opt}(t)$ it is optimal to hold it. In figure 2 we see that this is equivalent to projecting the intersection onto the $s \times t$ plane.

3 Numerical Pricing of the American Put

The problem of pricing an American put option has, as mentioned in section 2, no analytical solution. And thus no exact solution for the optimal exercise boundary. There are, however, ways to numerically determine the price of the option. In this section we will describe the numerical methods we have used to price the American put option and find the optimal exercise boundary.

3.1 Time discretization of the American Put

We have used the method described in [3]. Suppose that exercising only is allowed at n discrete points in time $[t, t + \Delta t, t + 2\Delta t, \ldots, T]$.

In this case, the option will behave like a European option with maturity date $(i + 1)\Delta t$ in each interval $i\Delta t < \tau < (i + 1)\Delta t,\ i = 0, \ldots, n - 1$. This enables us to price the option in $T - \Delta t$ using Theorem 2.2.

At this point exercising is allowed, and the option price will be the maximum of the just calculated price, f_{num}, and the exercise value $(K - s)^+$. Using this price we solve for the next time step using the same technique. We perform this repeatedly until we have reached our desired start date t. If we let $\Delta t \to 0$, the limit will be the price of the American put option.

The optimal exercise boundary is obtained by projecting the intersection between the price function and the contract function $(K - s)^+$ onto the $s \times t$-plane (see figures 1 and 2)

3.2 Numerical method

To solve the Black-Scholes equation numerically we use the implicit finite difference scheme Crank-Nicholson (see [8]). Using this we get an uncondi-

tionally stable method with an order of accuracy of (2,2) in time and space. The scheme is shown below, with time discretization step Δt and asset step Δs,

$$\frac{v_m^n - v_m^{n+1}}{\Delta t} + \frac{r s_m}{2}\left(\frac{v_{m+1}^n - v_{m-1}^n + v_{m+1}^{n+1} - v_{m-1}^{n+1}}{2\Delta s}\right) + \\ + \frac{\sigma^2 s_m^2}{4}\left(\frac{v_{m+1}^n - 2v_m^n + v_{m-1}^n + v_{m+1}^{n+1} - 2v_m^{n+1} + v_{m-1}^{n+1}}{\Delta s^2}\right) + \\ - r\left(\frac{v_m^n + v_m^{n+1}}{2}\right) = 0, \quad (7)$$

rearranging the terms gives us

$$\begin{aligned} v_{m-1}^{n+1}\left(\frac{r s_m \lambda}{4} - \frac{\sigma^2 s_m^2}{4}\right) + & \quad v_m^{n+1}\left(1 + \tfrac{\sigma^2 s_m^2 \mu}{2} + \tfrac{r\Delta t}{2}\right) + \\ + & \quad v_{m+1}^{n+1}\left(-\tfrac{\sigma^2 s_m^2 \mu}{4} - \tfrac{r s_m \lambda}{4}\right) = \\ = v_{m-1}^{n}\left(\frac{\sigma^2 s_m^2 \mu}{4} - \frac{r s_m \lambda}{4}\right) + & \quad v_m^{n}\left(1 - \tfrac{\sigma^2 s_m^2 \mu}{2} - \tfrac{r\Delta t}{2}\right) + \\ + & \quad v_{m+1}^{n}\left(\tfrac{\sigma^2 s_m^2 \mu}{4} + \tfrac{r s_m \lambda}{4}\right) \end{aligned} \quad (8)$$

with $\lambda = \frac{\Delta t}{\Delta s}$ and $\mu = \frac{\Delta t}{\Delta s^2}$. The time level is denoted by n and m is the asset grid-point.

The scheme (8) results in the system $Af_{num} = Mb$, where A and M are tridiagonal matrices, b is the known solution in the previous time step and f_{num} the unknown price at the present time. This system has to be solved in every time step. To do this efficiently we use Thomas Algorithm for tridiagonal systems ($\mathcal{O}(N)$ operations). Due to the heavy calculations needed, we implement all numerical calculations in FORTRAN90 . We use MATLAB for visualization and verification.

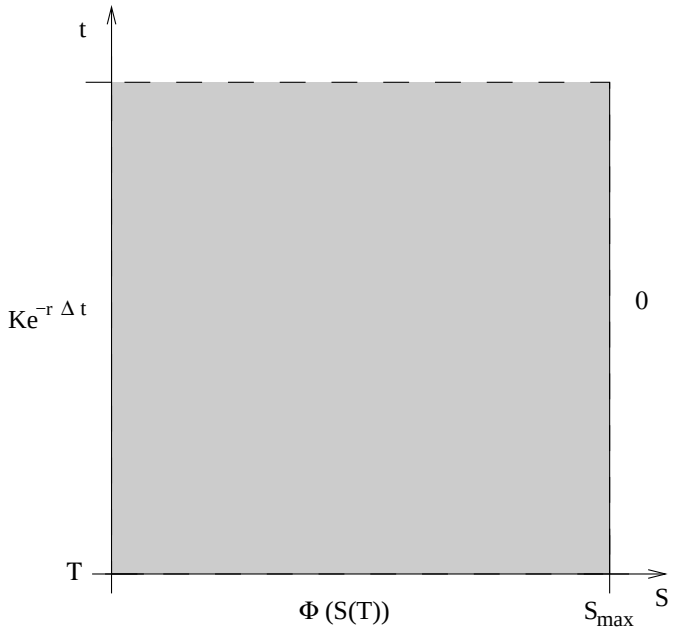

Figure 3: Computational area with boundary conditions.

3.3 Boundary Conditions

For the boundary $s = 0$ we chose the discounted exercise price $Ke^{-r\Delta t}$. The other boundary, analytically described by $f = 0$ as $s \to \infty$, has to be chosen artificially, denoted by s_{max}. The boundary conditions are illustrated in figure 3. Thus we set the point s_{max} sufficiently far from K and let $f = 0$ there, compare [9].

We noted that this choice played an important role in the accuracy of the far boundary results (see section 4.1). There, we had to use $s_{\max} = 9K$. But for the first five years the optimal exercise boundary is virtually the same for all selections of the artificial boundary and thus when we look at short maturities one can use $s_{\max} = 3K$. For a test with $\Delta s \sim 10^{-3}$ we got a maximum difference between $3K$ and $9K$ of the order 10^{-3} which is the expected accuracy (see section 3.4).

3.4 Finding the Optimal Exercise Boundary

We now have the problem of finding the intersection point of our solution f_{num} and the exercise price. This describes the optimal exercise boundary.

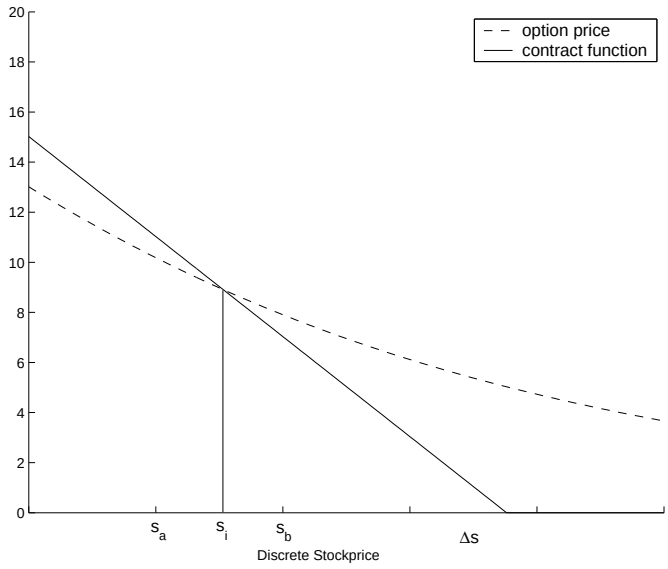

Figure 4: The point of intersection s_i is chosen as s_a or s_b depending of which one gives the smallest $|f_{num}(s) - (K-s)^+|$. We see that the order of accuracy is $\mathcal{O}(\Delta s)$ since s_a and s_b can differ from s_i with at most $\Delta s/2$

We do this by starting at a point $s_o > s_i$. This is possible since we know that the optimal exercise boundary, $f_{opt} < K$. After this we watch for a change in sign of $f_{num}(s) - (K - s)^+$ while stepwise decreasing s by Δs.

Having found this, we compare $|f_{num}(s) - (K - s)^+|$ for the points before (s_b) and after (s_a) the change of sign. The point that gives the smallest absolute difference is chosen as the point of intersection. See figure 4. Then we set $s_o = s_b$ as start value for the comparison in the next iteration, since we assume that the optimal exercise boundary is a convex function. (A reasonable assumption, had it been wrong we would not find a change of signs in the next iteration.) This procedure is performed repeatedly until we reach our desired start date.

3.5 Accuracy of the numerical method

We know that the Crank-Nicholson scheme has an order of accuracy of $\mathcal{O}(\Delta s^2, \Delta t^2)$. But the comparison function used to find the optimal exercise boundary gives rise to an other error in the asset space of at most $1/2\Delta s$. This leads to a total order of accuracy of $\mathcal{O}(\Delta s^2, \Delta t^2) + \mathcal{O}(\Delta s)$. And thus our method for finding the optimal exercise boundary has the accuracy $(1, 2)$

3.6 Performance

We have compiled our code with the command

`f90 -o name -fast -xtarget=ultra3plus -xarch=v9b filename.f90,`

where the flag `-xarch=v9b` is for 64-bit code with higher accuracy. The flag `-fast` is a macro that expands to

```
-xO5 -xpad=local -xvector=yes -xprefetch=auto,explicit -f
-fsimple=2 -fns=yes -ftrap=common -xlibmil -xlibmopt
-dalign -xdepend
```

and enables the compiler to use the highest level of optimization and to rearrange the code. It was executed on one serial processor on a machine with 16 GB of RAM.

n_s \ n_t	10^3	$5 \cdot 10^3$
10^5	$8.2s$	$41s$
10^6	$191s$	$1036s$

Table 1: Execution times for different problem sizes.

4 Optimal Exercise Analysis

When studying the optimal exercise boundary, we have concentrated on three main areas:

1. The properties far from maturity; i.e. the behavior as the expiry date $T \to \infty$.
2. The properties near maturity; i.e. how our numerical solutions compare to existing models of the asymptotical behavior near maturity.
3. Curve fitting of our numerical results; i.e. trying to find functions of r and σ that approximate the optimal exercise boundary.

4.1 Properties far from maturity

When the time to maturity tends to infinity the American put option converges to the *perpetual put*, an American put option with $T = \infty$. The optimal exercise boundary for such an option is known to be [7]

$$b^*_\infty = \frac{2rK}{2r + \sigma^2}. \tag{9}$$

We performed six tests with the artificial boundary at different positions ($s_{max} = cK$, $c = 3,\ 6,\ \ldots 18$) to see if this had any impact on the convergence. The results can be seen in table 2. Throughout these tests the number of space steps were constant and thus Δs increased in size.

We can see that as we increase c for the artificial boundary we get a better convergence towards the perpetual put

As mentioned in 3.3 the accuracy of our solution depended on where we chose to set the artificial boundary condition in each time step. However, this is only when the time to maturity $T - t > 4$: it is not until then that the solutions start to differ.

c	3	6	9	12	15	18
$f_{num} - b^*_\infty$	0.9697	0.4567	0.3091	0.3496	0.2920	0.2821

Table 2: Accuracy for the perpetual put, depending on where the artificial boundary condition is set (at $s_{max} = cK$)

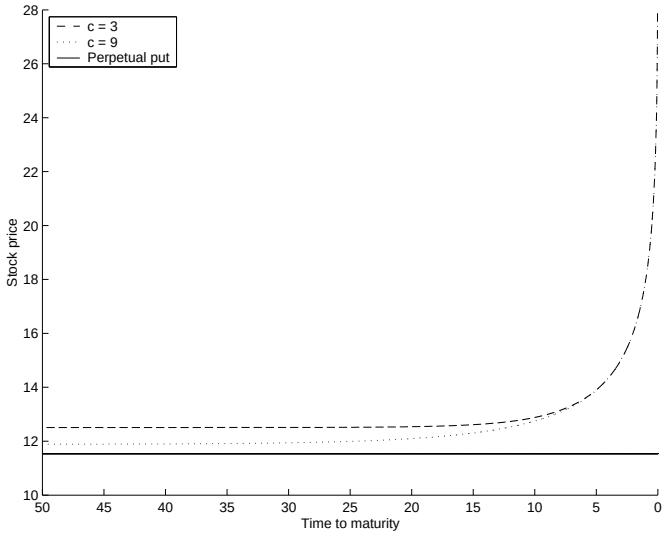

Figure 5: The numerical value of the American put option far from maturity compared to the theoretical value of the perpetual put for constant $\Delta t = 0.01$. Note the improvement when the artificial boundary (the stock price s_{max} that implies $F = 0$) is moved from $3K$ to $9K$.

This can be seen in figure 6, which shows differences between f_{opt} for different choices of s_{max}.

- $e_1 = f_{num}(s_{max} = 3K) - f_{num}(s_{max} = 9K)$
- $e_2 = f_{num}(s_{max} = 9K) - f_{num}(s_{max} = 12K)$
- $e_3 = f_{num}(s_{max} = 12K) - f_{num}(s_{max} = 18K)$

The mean for the difference, comparing s_{max} at $3K$ and $9K$, in the first 4 years is in the order of 10^{-3}.

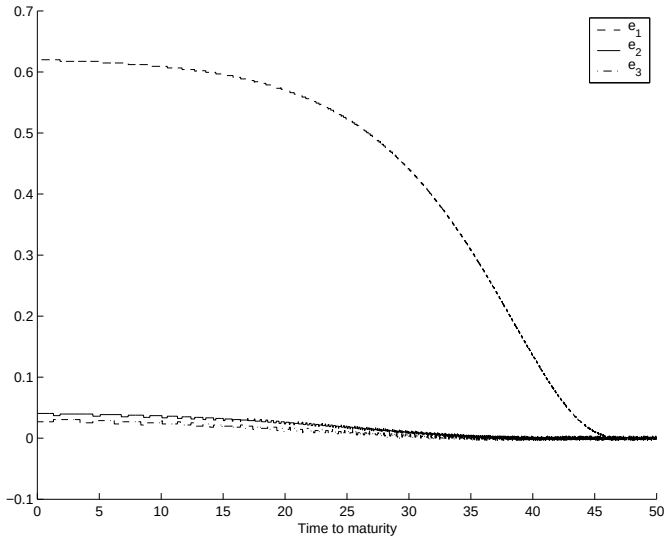

Figure 6: The difference between optimal exercise boundaries with the boundary condition set at different positions. The first five years the difference is $\mathcal{O}(\Delta s)$. When computing for maturities larger than five years, the choice of artificial boundary becomes more critical.

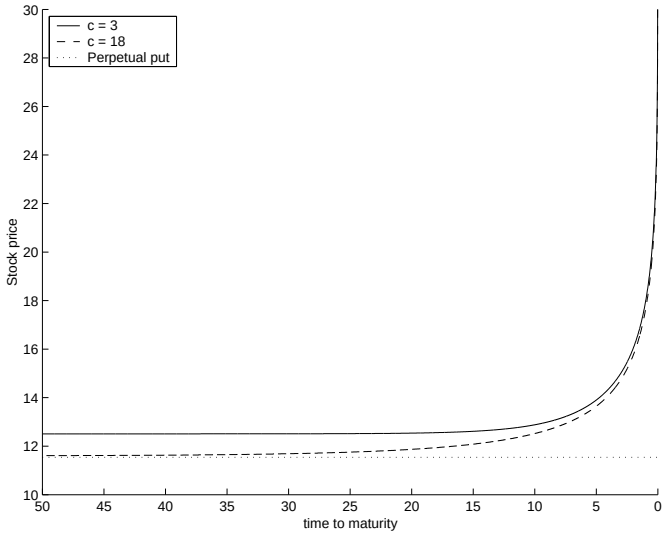

Figure 7: The numerical value of the American put option far from maturity compared to the theoretical value of the perpetual put. For $c = 3,\ , \Delta s = 0.0054,\ \Delta t = 0.01$ and for $c = 18,\ \Delta s = 9 \cdot 10^{-4},\ \Delta t = 0.0001$. Notice the big improvement with higher S_{max} and smaller Δt

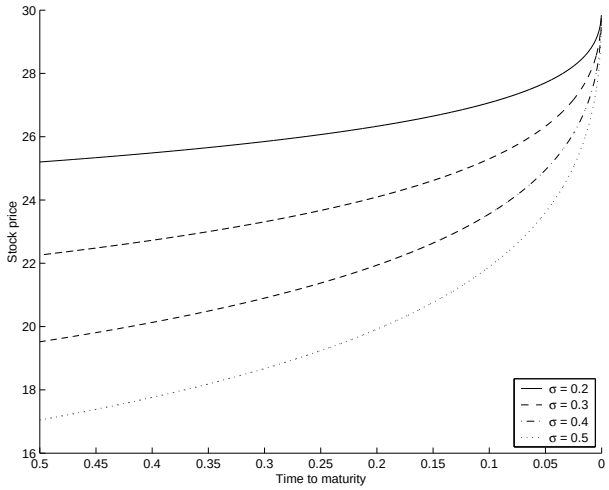

Figure 8: Impact on the near-maturity solution of varying the volatility.

4.2 Properties near maturity

Near maturity we compare our numerical results with known properties of the optimal exercise boundary. [6] states that the optimal exercise boundary

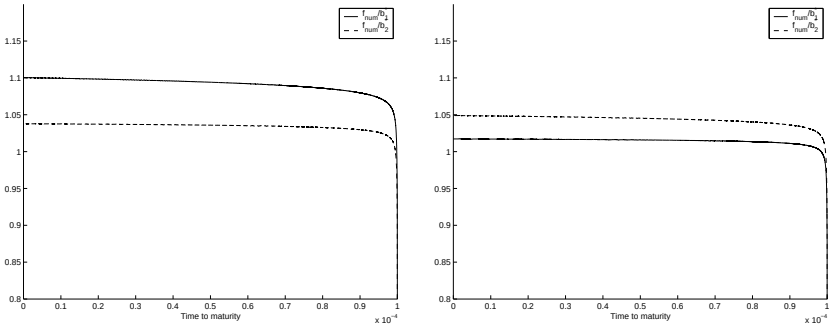

(a) $r = 0.03$ (b) $r = 0.07$

Figure 9: Numerical solution divided by the righthand-side of (10) and (11) for constant $\sigma = 0.4$

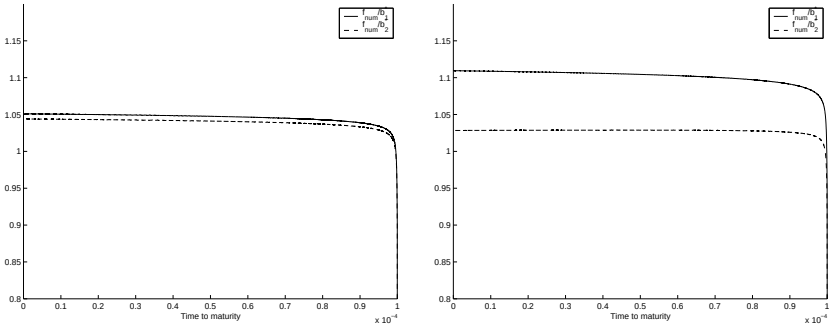

(a) $\sigma = 0.4$ (b) $\sigma = 0.8$

Figure 10: Numerical solution divided by the righthand-side of (10) and (11) for constant $r = 0.05$

$b^*(T-t)$ has an asymptotic behavior described by

$$b_1^*(T-t) \sim K(1 - \sigma\sqrt{(t-T)\ln(T-t)} \tag{10}$$

near the expiry date.

We also used a slightly more accurate expression given by [5]

$$b_2^*(T-t) \sim K\left(1 - \left[2\sigma^2(T-t)\ln\frac{\sigma\sqrt{2}}{6\pi^{1/2}r(T-t)^{1/2}}\right]^{1/2}\right). \tag{11}$$

The results can be seen in figures 9 and 10.

We can also see in figures 9(a)-10(b) that b_2^* is more stable than b_1^*. For $\sigma = 0.4$ and varying r the ratio b_2^* always stay close to 1.05 (except for the dip). b_1^* however varies a lot, for $r = 0.03$ we get $b_1^* \approx 1.1$ while for $r = 0.07$ we have $b_1^* \approx 1.02$.

If we change σ (figure 10(b)), the b_2^* ratio moves to ≈ 1.03. It is thus still fairly robust compared to b_1^*.

None of the ratios give a perfect result. Both vary with r and σ and none of them give the exact ratio of 1. One interesting note is that b_1^* varies a lot more than b_2^*. This is expected since b_2^* is a more accurate description.

4.3 Curve fitting of the numerical solution

Since there is no analytical expression for the optimal exercise boundary, it is of interest to find a function that approximates it. In our analysis, we try to find such functions when time to maturity $\tilde{t} = T - t < 0.5$.

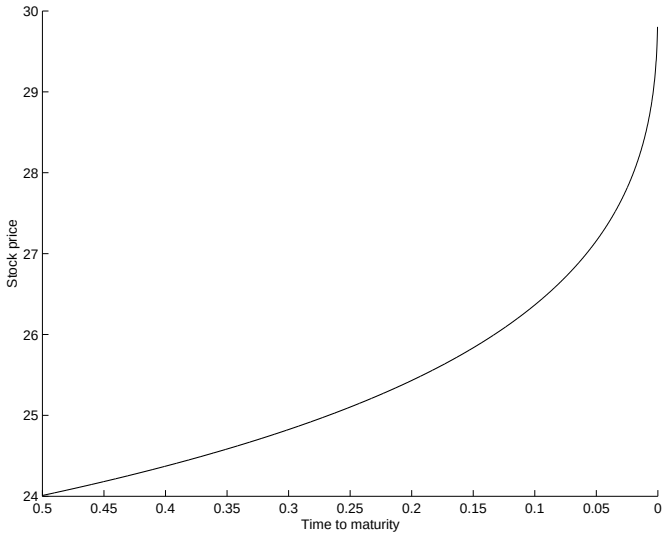

Figure 11: The optimal exercise boundary the last 6 months before expiry ($\sigma = 0.24$, $r = 0.05$). Near maturity, the slope of the boundary tends to infinity, which makes it difficult to fit a simple function to the data.

One of the more complicated properties of the optimal exercise boundary is that the time derivative of the optimal exercise boundary goes to infinity as

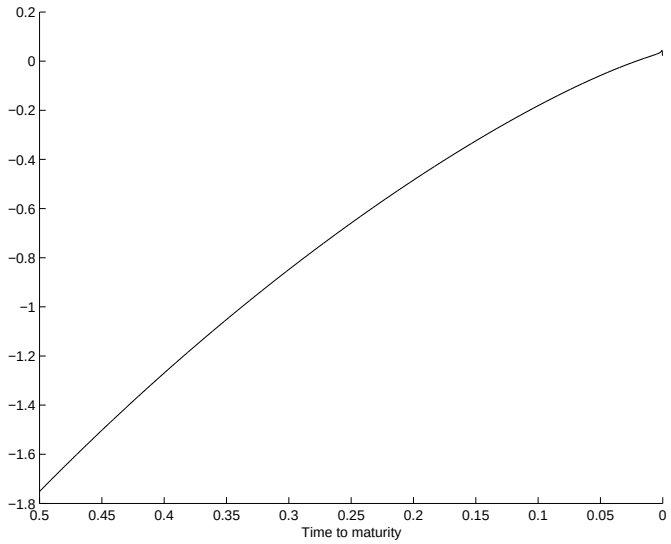

Figure 12: The optimal exercise boundary with the analytical asymptotical boundary b_1^* subtracted ($\sigma = 0.24$, $r = 0.05$). A polynomial of some degree can be fitted to this data.

the expiry date approaches (see figure 11). To avoid this problem, we subtract the simpler asymptotic expression (10) from our numerical solution:

$$\tilde{f}_{num} = f_{num} - b_1^*$$

and the resulting curve is shown in figure 12. The reason of choosing b_1^* instead of b_2^* is that b_1^* is always real-valued during the last year before expiry. b_2^* is real-valued for intervals that depend on σ and r and is therefore not practical when comparing results with varying parameters.

We can see in figure 12 that this curve looks much simpler than the previous. It can be fitted in a least squares sense to some polynomial.

Our idea is to first use polynomials in $\tilde{t}$ to approximate the curves for each σ. Using this approximation we combine these polynomials into a new polynomial with σ-dependent coefficients, i.e. an expression on the form

$$a_n(\sigma)\tilde{t}^n + a_{n-1}(\sigma)\tilde{t}^{n-1} + \ldots + a_1(\sigma)\tilde{t} + a_0(\sigma). \tag{12}$$

The coefficients can be expressed as polynomials in σ as seen in figure 13. This gives us a general expression for a_i, $i = 0, \ldots, n$

$$a_i(\sigma) = \alpha_m\sigma^m + \alpha_{m-1}\sigma^{m-1} + \ldots + \alpha_1\sigma + \alpha_0 \tag{13}$$

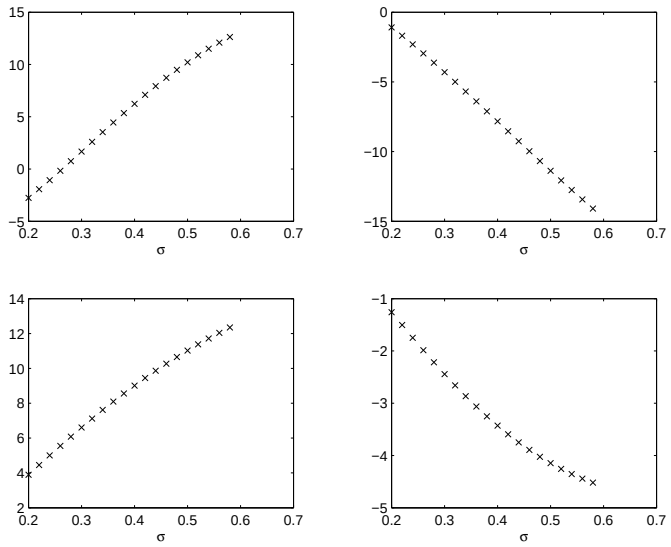

Figure 13: The coefficients of polynomials of degree three plotted against σ. The points can be described with good precision using polynomials of degree two.

where α_i, $i = 0, \ldots, m$ are constants.

We vary σ in the interval $0.2 < \sigma < 0.6$ while keeping all other parameters constant, with $T = 0.5$ years and $r = 0.05$. For each σ we fit an n-th degree polynomial to $\tilde{f}_{num}$ and get $n + 1$ coefficients. Then we fit an m-th degree polynomial in σ to each of these n coefficients, resulting in a total of $n \cdot m$ coefficients. An example is given in table 5

As can be seen in tables 3 and 4, the accuracy is only slightly improved by choosing the degree of the polynomials in a (d_a) and b, (d_b) higher than 2.

We now try the same strategy when holding σ constant and varying r. The expression we are looking for is similar to (14),

$$p(t) = b_n(r)\tilde{t}^n + b_{n-1}(r)\tilde{t}^{n-1} + \ldots + b_1(r)\tilde{t} + b_0(r). \tag{14}$$

First we find polynomials in $\tilde{t}$, which gives us an error comparable with the first polynomial approximation above in the σ-case. When trying to find the coefficient functions b_i, $i = 0, \ldots, n$, we find that they are harder to approximate than above (see figure 15(a)). If these values are instead plotted against $\ln r$, see figure 15(b), we see that the coefficients can be approximated with polynomials in $\ln r$, i.e.

$$b_i((\ln r)) = \beta_m(\ln r)^m + \beta_{m-1}(\ln r)^{m-1} + \ldots + \beta_1(\ln r) + \beta_0 \tag{15}$$

d_p \ d_a	1	2	3	4	5	6
1	0.2418	0.1729	0.1734	0.1733	0.1733	0.1733
2	0.2075	0.1748	0.1742	0.1742	0.1742	0.1742
3	0.1717	0.1363	0.1359	0.1358	0.1359	0.1359
4	0.1624	0.1117	0.1113	0.1113	0.1113	0.1113
5	0.1494	0.0916	0.0913	0.0913	0.0913	0.0913
6	0.1455	0.0762	0.0760	0.0760	0.0760	0.0760
7	0.1394	0.0641	0.0639	0.0639	0.0639	0.0639
8	0.1377	0.0544	0.0542	0.0542	0.0542	0.0542
9	0.1348	0.0467	0.0466	0.0466	0.0466	0.0466
10	0.1344	0.0405	0.0403	0.0403	0.0403	0.0403

Table 3: Errors in the fitting of $\tilde{f}_{num}$ with polynomials of various degrees ($d_p = \deg[p(t)],\ d_a = \deg[a(\sigma)]$).

d_p \ d_b	1	2	3	4	5	6
1	0.5706	0.5583	0.5572	0.5570	0.5571	0.5571
2	0.2965	0.2896	0.2893	0.2893	0.2893	0.2893
3	0.2101	0.2014	0.2012	0.2012	0.2012	0.2012
4	0.1601	0.1505	0.1504	0.1504	0.1504	0.1504
5	0.1335	0.1191	0.1190	0.1190	0.1190	0.1190
6	0.1143	0.0976	0.0975	0.0975	0.0975	0.0975
7	0.1019	0.0822	0.0822	0.0822	0.0822	0.0822
8	0.0919	0.0707	0.0706	0.0706	0.0706	0.0706
9	0.0849	0.0618	0.0617	0.0617	0.0617	0.0617
10	0.0788	0.0549	0.0546	0.0546	0.0546	0.0546

Table 4: Errors in the fitting of $\tilde{f}_{num}$ with polynomials of various degrees ($d_p = \deg[p(t)],\ d_b = \deg[b(r)]$).

where $\beta_i,\ i = 0, \ldots, m$ are constants.

For a number of constant r's we vary σ, creating a mesh over the $r \times \sigma$-plane. We can then perform the first step of our polynomial approximation for each of the combinations of σ and r. The approximations can be used to see how the polynomial coefficients depend on our two variables. In figure 4.3 we can see an example of the coefficient surfaces obtained in this experiment for a third degree approximation.

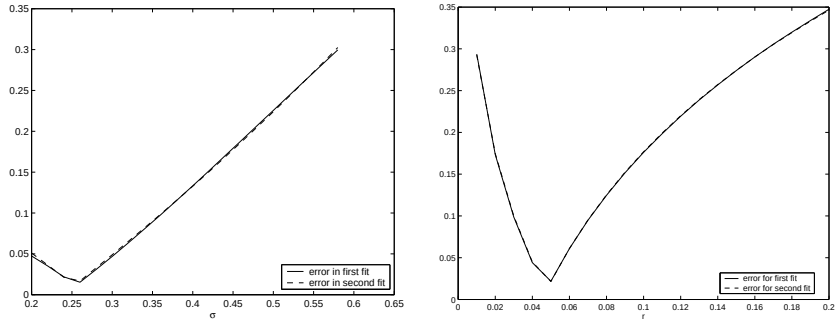

(a) Error for varying σ (b) Error for varying r

Figure 14: Error for the polynomial fittings with varied σ and r. In this example we use $d_p = \deg[p(t)] = 3,\ \deg[a(\sigma)] = \deg[b(r)] = 2$

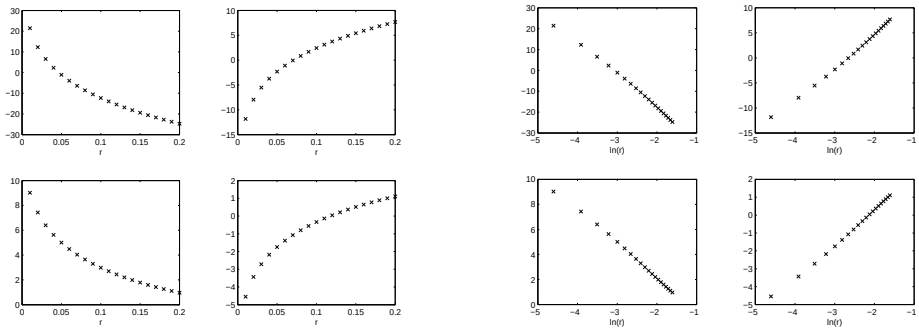

(a) (b)

Figure 15: The coefficients of polynomials of degree three plotted against r (figure (a)) and $\ln(r)$ (figure (b)). The points in (b) can be described by polynomials of degree two.

	α_2	α_1	α_0
a_3	-23.8479	61.3401	-14.3814
a_2	-3.4041	-32.7234	5.7284
a_1	-18.5638	36.9310	-2.7823
a_0	12.5883	-18.4963	1.9609

Table 5: Coefficients for a polynomial.

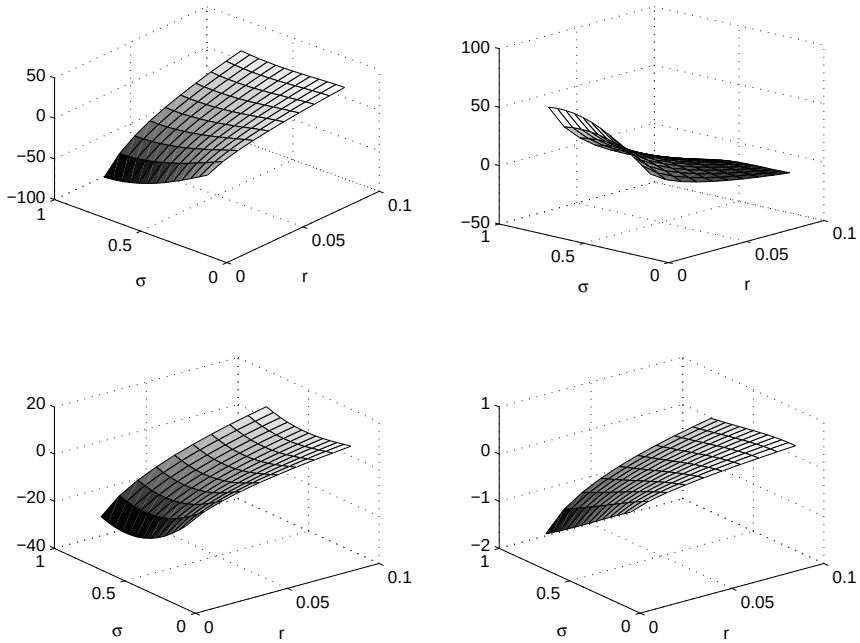

Figure 16: The coefficients of a third degree polynomial in $\tilde{t}$ with respect to their values of σ and r.

5 Discussion

We were able to investigate a lot of interesting features of the American put option. Though the project deadline set a limit to how deep into each subject we were able to analyze. The conclusions we did make are discussed in this chapter.

5.1 Far from maturity

The most interesting result is where to put the artificial boundary s_{max}. Most options have maturities of at most half a year. So using the results of section 4.1, it is sufficient to have $s_{max} = 3K$ to get a good accuracy for the first 4 years to maturity.

By combining a large s_{max} with a short time step (which of course increases the accuracy) we where able to get as close as 0.07 to b^*_∞ (see (9)). By further increasing s_{max} and decreasing Δt we should be able to get even closer to the perpetual put.

5.2 Near maturity

The dip in our results could be due to a number of numerical errors. We have a discontinuous derivative in the point $S = K$ which creates a chock that propagates throughout the solution.

Fortunately, the properties of the differential equation in theorem 2.2 is that of a diffusion equation which has a dampening effect. We thus get dissipative qualities in our numerical scheme and the the chock will be smoothened after a few iterations. During the first iterations though the chock will have effect and this may give rise to the dip.

5.3 Curve fitting

Since there is no analytical expression for the optimal exercise boundary, it would be very useful if we could find an approximative expression to it, say a quadratic function of r and σ, given some error tolerance.

We have this far only obtained results for the case when one of the parameters is constant. An interesting next step would be to make a more in-depth study on surfaces like the ones in figure 4.3 to generate more general results.

References

[1] Tomas Björk. *Arbitrage Theory in Continuous Time*. Oxford University Press, 1998.

[2] Tom Coleman. Numerical solution of black-scholes equation, 1998. Lecture Notes for CS 522: Computational Tools and Methods for Finance (Spring 1998),Department of Computer Science, Cornell University.

[3] Jonathan Goodman, Kyoung-Sook Moon, Anders Szepessy, Raúl Tempone, and Georgios Zouraris. Stochastic and partial differential equations with adapted numerics, January 2002. Lecture notes for Mathematical Models, Analysis and Simulation, Part II, Royal Institute of Technology, Stockholm, Sweden.

[4] Raul Kangro and Roy Nicolaides. Far field boundary conditions for Black-Scholes equations. *SIAM J. Numer. Anal.*, 38(4):1357–1368 (electronic), 2000.

[5] Rachel Kuske and Joseph B. Keller. Optimal exercise boundary for an american put option. *Applied Mathematical Finance*, 5:107–116, 1998.

[6] Damien Lamberton. Critical price for an American option near maturity. In *Seminar on Stochastic Analysis, Random Fields and Applications (Ascona, 1993)*, pages 353–358. Birkhäuser, Basel, 1995.

[7] Marek Musiela and Marek Rutkowski. *Martingale methods in financial modelling*. Springer-Verlag, Berlin, 1997.

[8] C. Vázquez. An upwind numerical approach for an American and European option pricing model. *Appl. Math. Comput.*, 97(2-3):273–286, 1998.

[9] Lixin Wu and Yuk-Kuen Kwok. A front-fixing finite difference method for the valuation of american options. *Journal of Financial Engineering*, 6(2):83–97, 1997.